High reflectivity large scale telescope mirror coatings via long throw sputtering

A. J. Bourque and J. H. Gurian

Dynavac, 110 Industrial Park Road, Hingham, MA 02043, USA

May 26, 2014

ABSTRACT

Here we present reflectivity measurements of long throw sputtered aluminum coatings at normal and oblique incidence angles on glass test chips. Experimental results indicate that water vapor partial pressure, not incident angle, is the dominant factor for front surface reflectivity of sputtered aluminum. These results highlight the importance of water vapor pumping in telescope mirror coating vacuum chambers and indicate that long-throw sputtering is an economical and reliable technique for producing high uniformity, high reflectivity mirror coatings across large substrates.

Keywords: Mirrors, Optical Coatings, Aluminum, Sputtering, Sputter Deposition, Long-throw sputtering

1. INTRODUCTION

The upcoming generation of large scale telescopes will require highly uniform, highly reflective, durable mirrors with substrate diameters greater than eight meters. Evaporative coatings have traditionally required a high deposition rate and broad source coverage to successfully evaporate a reflective coating.[1,2] Furthermore, great pains are usually taken to avoid oblique angle evaporation which can lead to the growth of columnar structures, reducing reflectivity.[3–5]

Recently, there has been increased interest in applying newer technologies to telescope mirror coatings, such as magnetron sputtering. Sputtering provides an attractive solution for single and multilayer reflective coatings across large substrates. However, short-throw sputtering requires a greater initial expense, increased facility utility needs, and requires advanced masking to compensate for mirror curvature.[6] Long throw sputtering, a popular technique for semiconductor processes,[7,8] offers improved density and coating adhesion compared to evaporated coatings, while producing highly uniform coatings across the entire mirror curvature with minimal masking required.

While very successful throughout the world of semiconductor manufacturing and successfully applied to produce silver coated astronomical mirrors,[9] long throw sputtering of aluminum has not yet been successfully applied to large scale telescope applications.[10,11] Previous aluminum sputtering tests have raised concerns about the broad angular distribution of long throw sputtering and its impact on Al mirror reflectivity, particularly at the annular joint of a coating, or "seam", of a mirror coated in a circular fashion.[12]

Here we present a series of experiments to determine the impact of various long-throw sputtering parameters to mirror reflectivity compared to a standard commercially available front surface aluminum mirror. We will describe our experimental approach, present our results, and comment on their implications in the sections that follow.

2. EXPERIMENTAL APPROACH

All experiments were conducted in a standard Dynavac 36" optical coating system, using two different experimental configurations. The first utilizes two 2" diameter Materials Science Polaris Gen II magnetron sputtering sources. The first magnetron ("Magnetron 1") is mounted vertically to sputter material on horizontal glass test slides (25 mm x 75 mm) fixed 30 cm directly above the magnetron. The second magnetron ("Magnetron 2") is mounted in the same horizontal plane as the first magnetron, 40 cm from Magnetron 1. Magnetron 2 is tilted towards the glass slide to maximize rate at a $\sim 53^\circ$ incidence angle. Both magnetrons use 1100 aluminum sputtering targets and MKS 1179A mass flow controllers to control the flow of argon gas to the magnetrons. A basic diagram of the chamber setup is shown in Fig. 1. Power for

Corresponding author: jgurian@dynavac.com

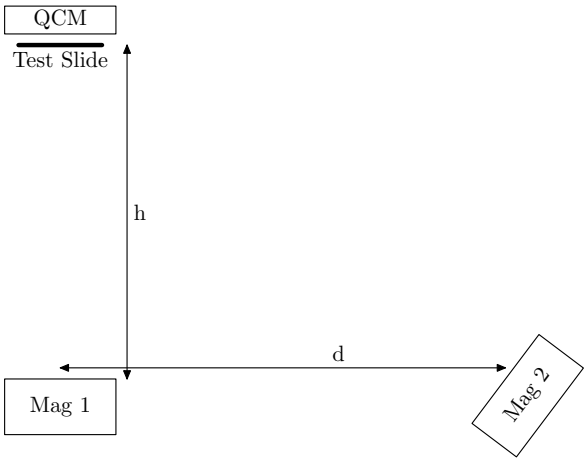

Figure 1. Side schematic of Experimental setup 1. Two magnetrons are mounted in a plane h=30 cm below a horizontal glass slide and quartz crystal monitor (QCM) sensor. The second magnetron, labeled "Mag2", is a distance d=40 cm from the first magnetron (labeled "Mag1").

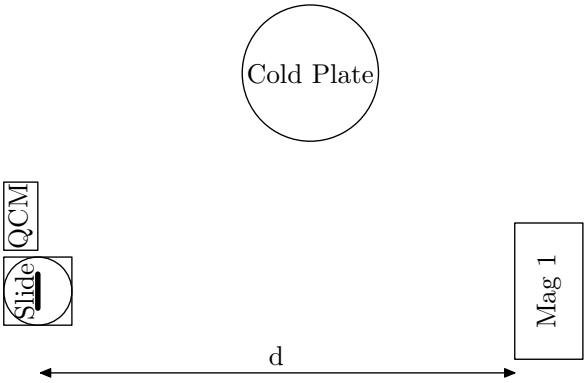

Figure 2. Overhead schematic of Experimental setup 2. A single magnetron is mounted horizontally in the chamber, d=72.4 cm from a test slide. The test slide is affixed upright to a small rotation stage to allow for angular rotation of the test slide with respect to the sputtering source. A 180 mm diameter LN_2 cold plate mounted below the plane of the magnetron and test slide provides additional water vapor pumping. The quartz crystal monitor (QCM) sensor is mounting next to the test slide, at the same source to substrate distance as the test slide.

the magnetrons is provided by an Advanced Energy 5 kW MDX power supply, and the deposition process is controlled via Dynavac's Labview based control software. The deposition rate is measured using a standard Inficon 6 MHz Front Load Dual Quartz Crystal Monitor (QCM) mounted directly next to the glass slide in the same horizontal plane. The QCM is controlled by an Inficon IC/5 Thin Film Deposition Controller. The system is pumped via a single Brooks CTI-Cryogenics OB-400 cryopump to provide approximately 11 m^3/sec of net water vapor pumping to the system. Additionally, a 180 mm diameter liquid nitrogen cold plate is installed inside the chamber for an optional additional 8 m^3/sec of water vapor cryopumping. All vacuum gauging is measured using an Instrutech IGM402 Hornet Hot Cathode Bayard-Alpert ionization gauge with attached CVG101 Worker Bee convection enhanced Pirani gauge.

The second experimental test setup utilizes a single magnetron source. A 2" diameter Materials Science Polaris Gen II magnetron sputtering source is horizontally mounted in the system to provide a d=72.4 cm throw distance. A 99.999% pure aluminum target is installed in the magnetron. Glass slides (25mm x 75mm) are mounted vertically in the chamber on a same-sized mounting bracket using Kapton tape. The mounting bracket is set on a ThorLabs MSRP01/M Mini-Series rotation platform to precisely control the incident angle relative to the fixed sputtering cathode position. A diagram of the experimental setup is shown in Fig. 2.

An Ametek Dycor Dymaxion 50 amu Residual Gas Analyzer (RGA) is mounted to the chamber to provide background gas characterization. Two example scans are shown in Fig. 3. The RGA integrated total pressure and the hot cathode ion

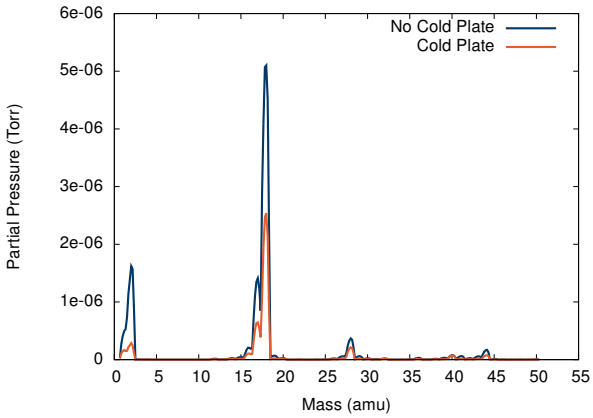

Figure 3. Two example Residual Gas Analyzer (RGA) scans, with (orange) and without (blue) the LN_2 cold plate operating. The most prominent peak in both scans, H_2O^+ ions at 18 amu, decreases by a factor of two when the cold plate is below -140 °C.

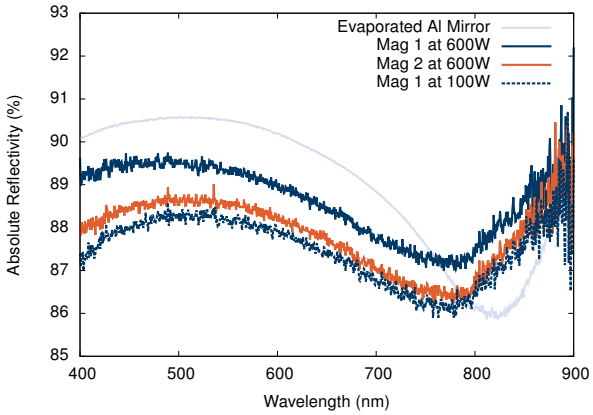

Figure 4. Comparison of the reflectivity of coatings produced by Magnetron 1 at 600 W and Magnetron 2 at 600 W. The longer throw distance decreases the deposition rate by a factor of five (greater than a r^{-2} assumption would suggest). Operating Magnetron 1 at a similar lower deposition rate produces a similar reduction in reflectivity. The reflectance of the baseline evaporated front surface aluminum mirror is shown in gray.

gauge are rarely in agreement, with the partial pressure of water measured by the RGA often higher than the total pressure measured by the ion gauge.

3. OBSERVATIONS

All test slide deposition thicknesses are measured by a Tencor Alphastep 200 automatic step profiler. All test slides are subjected to an adhesion "tape-test", of which no test slide failed. Sputtered reflectivity measurements are done using a Shimadzu UV-2401PC UV-Vis Recording Spectrophotometer with a Harrick Near-Normal Incidence Specular Reflection Attachment over wavelengths from 400 nm to 900 nm. All test slide reflectance measurements are normalized to a single commercial aluminum front surface mirror. Absolute reflectance measurement of the commercial aluminum front surface mirror was conducted on an Agilent Cary 5000 spectrophotometer by Evaporated Coatings, Inc. Absolute reflectance measurements were further corrected at 635 nm at Dynavac using a Thorlabs CPS180 1 mW diode laser measured with a Thorlabs DET36A biased Si photo-detector to 89.8 % average absolute reflectance (both polarizations averaged, 8° angle of incidence).

Using the first experimental setup, initial tests looked to establish whether there was a decrease in reflectivity when long-throw sputtering at high incidence angles. The results are shown in Fig. 4. Magnetron 1 was operated at a constant 600 W of power with 35 sccm of argon flowing to the cathode. The chamber pressure during deposition was 2×10^{-4} Torr, and an average deposition rate of 2.08 Å/sec was measured on the crystal monitor during a 100 nm deposition. The relative reflectivity is plotted as the blue curve in Fig. 4. Magnetron 2 was operated with the same parameters, with the test slide

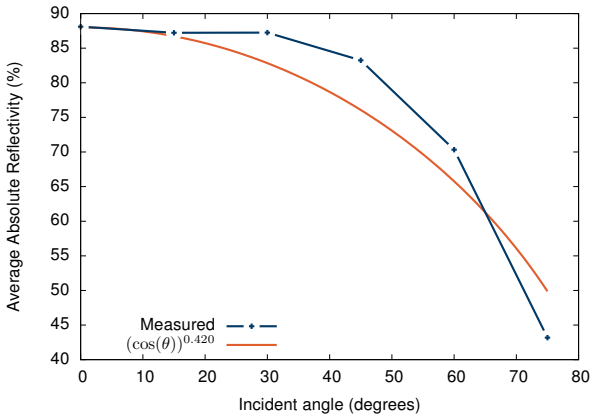

Figure 5. Reflectivity as a function of incident angle, averaged across 400 nm to 900 nm. Orange curve shows best single variable fit, $(\cos\theta)^n$.

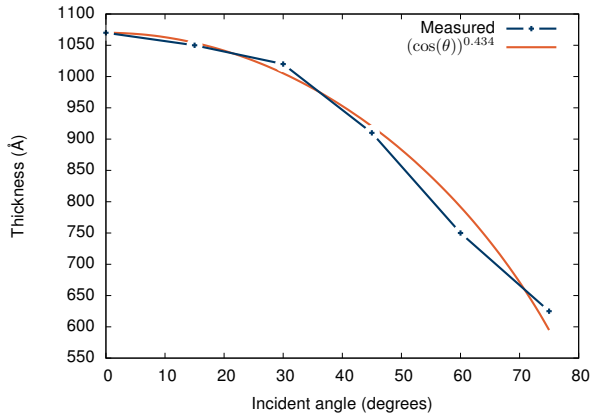

Figure 6. Deposition thickness as a function of incident angle. Deposition for each test slide stopped when the quartz crystal monitor thickness was measured to be 1000 Å. Thicknesses slightly greater than 1000 Å indicate that the quartz crystal monitor was slightly off-axis from the output of the magnetron compared to the test slide. The orange curve shows best single variable fit, $(\cos\theta)^n$.

reflectivity shown as the orange curve. A slightly greater than 1 % decrease in relative reflectivity is measured. However, due to the increased source to substrate distance, the deposition rate decreased by more than a factor of five, to 0.39 Å/sec. Consequently, the deposition time extended from 8 minutes to 42 minutes for a 100 nm deposition. Subsequently, Magnetron 1 was operated at a lower constant power, 100 W, to recreate a similar lower deposition rate. Depositing 100 nm of aluminum at an average rate of 0.37 Å/sec (45 minutes) resulting in a test slide with a slightly lower reflectivity, shown in dashed blue, than the angled deposition from Magnetron 2. Similar experiments were conducted at a higher sputtering pressure (7×10^{-4} Torr, 65 sccm argon) with equivalent results. The decrease in reflectivity with decreasing rate indicates that particles other than aluminum are mixing into the reflective coating. The blue RGA scan of Fig. 3 would indicate that water vapor is the most likely culprit, and that the chamber would benefit from additional water vapor pumping.

Experimental Setup 2 allowed us to investigate the change in reflectivity with angle and ensure a constant incident rate of aluminum. Using the crystal monitor mounted next to the test slide, 1000 Å of Al was emitted from the magnetron operating at 1000 W with an average deposition rate of 0.5 Å/sec on the crystal sensor. Coating runs produced test slides coated at constant incident angles of 0 degrees to 75 degrees, and the average reflectivity results from 400 nm to 900 nm are shown in Fig. 5.

While the reflectivity decreases as the incident angle increases, the measured thickness of deposited aluminum on the test slides also decreases with increasing incident angle. A plot of the measured thickness versus incident angle is shown in Fig. 6. Further testing is required to extrapolate the exact relationship between incident angle and reflectivity independent of thickness and deposition rate.

The results of Experimental Setup 1, where a slow deposition directly underneath a test slide produces a less reflective

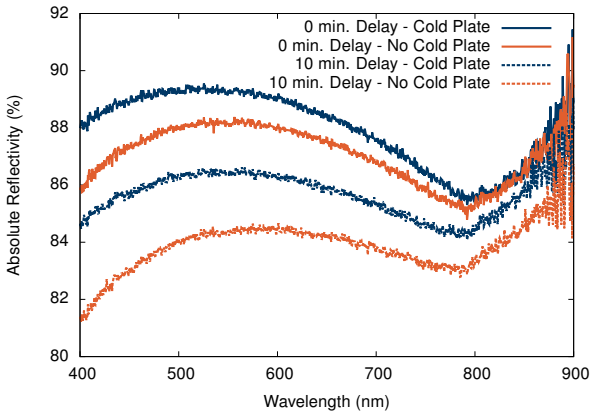

Figure 7. Reflectivity of 1000 Å samples, deposited either as continuously (solid curves) or with a ten minute delay (dotted curves) in deposition at 800 Å. Blue curves include an additional estimated 8 m^3/sec of water vapor pumping via a 180 mm diameter LN_2 cold plate. Reflectivity, particularly for bluer wavelengths, is improved with additional water vapor pumping.

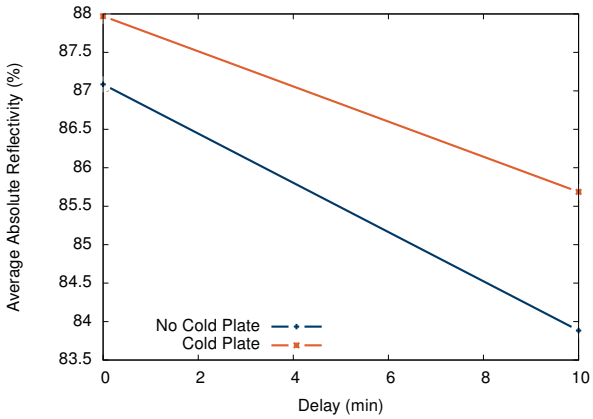

Figure 8. Reflectivity of annular joint samples as a function of delay between first and second layers. The first layer is stopped at 80 Å and the second layer is 20 Å. Additional water vapor pumping improves the reflectivity of both the base coating and the annular joint ("seam").

coating than an angled deposition coating, imply that incidence angle may not be the driving concern when coating large telescope mirrors. With that in mind, a set of coatings were produced using Experimental Setup 2, with a pause taken during deposition. This was intended to mimic the "seam" of a circularly coated large telescope mirror. Test slides were coated at normal incidence at an average rate of 0.38 Å/sec (600-720 W, dependent on target lifetime) with an ion gauge chamber baseline pressure between 1.2×10^{-6} Torr and 4×10^{-6} Torr and a sputtering pressure of 2.3×10^{-4} Torr (40 sccm argon). For two tests, one with the cold plate at 22 °C and the other with the cold plate at -181 °C, 100 nm of aluminum was deposited on a test slide. For two more tests, 80 nm of aluminum was deposited, the magnetron was turned off for ten minutes, and the remaining 20 nm was then deposited on the test slide. The reflectivity results of these tests are shown in Fig. 7. The reflectivity curves with the cold plate at room temperature are shown in orange, and the cold plate filled with LN_2 results are plotted in blue.

By averaging the reflectivity of each test slide across the measured wavelength range, 400 nm to 900 nm, we can more easily observe the influence of additional water vapor pumping in the system. These averaged reflectivities are plotted in Fig. 8 as a function of delay time. Additional water vapor pumping clearly improves the reflectivity of the zero delay mirror, and also improves the degradation of the 80 % annular joint. With only the cryopump, we see an annular joint reflectivity degradation of 0.358 %/minute. Including the cold plate reduces the seam degradation to 0.255 %/minute. This 30 % performance improvement comes from a roughly 50 % decrease in water vapor partial pressure. We hypothesize that annular joint issues in aluminum coatings stem from a water vapor interlayer developing between the initially and finally deposited aluminum that degrades reflectivity, and reduction of the partial pressure of water vapor to the 10^{-8} Torr regime should remove any reflectivity issues. This result provides a strong argument for including large amounts of water vapor

pumping in aluminum short and long throw sputtering chambers to avoid annular joint reflectivity issues.

4. CONCLUSION

In conclusion, we have measured the reflectivity of long-throw sputtered coatings at normal and high incidence angles, and at varying amount of water vapor pumping. Taken together, these results suggest that water vapor control is the dominant factor in producing highly reflective durable aluminum mirror coatings, and that long throw sputtering in a low water partial pressure environment can be extremely successful.

ACKNOWLEDGMENTS

It is a pleasure to acknowledge fruitful discussions with T. P. Foley, R. A. Crocker, S. J. Chiavaroli, G. S. Ash and M. Boccas. Thanks to R. Schaffer of Evaporated Coatings, Inc. for arranging an absolute reflectance measurement of our baseline mirror.

REFERENCES

[1] Hass, G., "Filmed surfaces for reflecting optics," *J. Opt. Soc. Am.* **45**, 945–952 (Nov 1955).

[2] Hass, G. and Waylonis, J. E., "Optical constants and reflectance and transmittance of evaporated aluminum in the visible and ultraviolet," *J. Opt. Soc. Am.* **51**, 719–722 (Jul 1961).

[3] Holland, L., "The effect of vapor incidence on the structure of evaporated aluminum films," *J. Opt. Soc. Am.* **43**, 376–380 (May 1953).

[4] Kivaisi, R., "Optical properties of obliquely evaporated aluminium films," *Thin Solid Films* **97**(2), 153 – 163 (1982).

[5] Dirks, A. and Leamy, H., "Columnar microstructure in vapor-deposited thin films," *Thin Solid Films* **47**(3), 219 – 233 (1977).

[6] Boccas, M., Vucina, T., Araya, C., Vera, E., and Ahhee, C., "Coating the 8-m gemini telescopes with protected silver," *Proc. SPIE* **5494**, 239–253 (2004).

[7] Rossnagel, S., "Sputter deposition for semiconductor manufacturing," *IBM Journal of Research and Development* **43**(1.2), 163–179 (1999).

[8] Motegi, N., Kashimoto, Y., Nagatani, K., Takahashi, S., Kondo, T., Mizusawa, Y., and Nakayama, I., "Long-throw low-pressure sputtering technology for very large-scale integrated devices," *Journal of Vacuum Science Technology B: Microelectronics and Nanometer Structures* **13**(4), 1906–1909 (1995).

[9] Wolfe, J. D., Sanders, D. M., Bryan, S., and Thomas, N. L., "Deposition of durable wide-band silver mirror coatings using long-throw, low-pressure, dc-pulsed magnetron sputtering," *Proc. SPIE* **4842**, 343–351 (2003).

[10] Boccas, M., "Summary of various tips and conclusions obtained in the 2002 al coating campaign at gs and the visit by mike plaisted (soleras)," tech. rep., Gemini 8-M Telescopes Project (October 2009).

[11] Boccas, M., "Coating tests done of 7th of may 2002," tech. rep., Gemini 8-M Telescopes Project (2003).

[12] Boccas, M., "Private communication," RE: GMTO PDR last week (November 2013).